

Review

Hypothesis: spring-loaded boomerang mechanism of influenza hemagglutinin-mediated membrane fusion

Lukas K. Tamm*

Department of Molecular Physiology and Biological Physics, University of Virginia Health Sciences Center, 1300 Jefferson Park Avenue,
P.O. Box 800736, Charlottesville, VA 22908-0736, USA

Received 28 April 2003; accepted 15 May 2003

Abstract

Substantial progress has been made in recent years to augment the current understanding of structures and interactions that promote viral membrane fusion. This progress is reviewed with a particular emphasis on recently determined structures of viral fusion domains and their interactions with lipid membranes. The results from the different structural and thermodynamic experimental approaches are synthesized into a new proposed mechanism, termed the “spring-loaded boomerang” mechanism of membrane fusion, which is presented here as a hypothesis.

© 2003 Elsevier B.V. All rights reserved.

Keywords: Membrane fusion; Fusion peptide; Hemagglutinin; Structure; Folding; Energetic; Lipid–protein interaction

1. Introduction

Enveloped viruses enter cells by membrane fusion. Thanks to evolution, viruses accomplish this task by the use of specialized envelope glycoproteins, i.e. fusion proteins, that cooperate to form a sophisticated molecular machine to merge viral and cellular target membranes without losing contents to the environment. Much insight into how these molecular machines work has been gleaned from X-ray crystallographic studies of the soluble ectodomains of several viral fusion proteins [1]. The common theme that has emerged from these structural studies is that class I¹ fusion proteins consist of three identical subunits that fold into long trimeric coiled coils of α -helices along the threefold symmetry axis of the core structure. These core coiled coils are surrounded by a second layer of three shorter α -helices that are oriented antiparallel to the central helices.

The hemagglutinin (HA) of influenza virus has long served as the paradigm viral fusion protein. Influenza HA gained this prominent role because its structure was solved in pioneering work more than 20 years ago [2]. Each subunit of the HA trimer contains two polypeptide chains, HA1 and HA2. The HA1 chains harbor the receptor binding sites for virus attachment to the cell surface. The HA2 chains are thought to be primarily responsible for the fusion activity. Unlike some other viruses that fuse at neutral pH directly with the cell membrane, influenza virus first enters cells as an intact particle by receptor-mediated endocytosis. Fusion is then triggered by the mildly acidic pH (around 5) that prevails in the endosome. Remarkably, the structure of HA refolds completely in response to this pH change [3]. Although it is known that the trimer contacts between HA1 subunits are loosened upon activation by pH 5 [4,5], the low-pH structures of these subunits are not known (but see Ref. [6] for a structure of the HA1 monomer at pH 6). The bundles of coiled coils discussed above are part of the HA2 polypeptide chains. In the crystallographically observed refolding reaction [3], only the top (N-terminal) halves of the central coiled coils remain intact. The bottom (C-terminal) halves break off, form a tight 180° turn, and pack antiparallel against the core helices. In contrast, the original antiparallel outer helices, which at neutral pH are connected by long extended loops to the top ends of the

* Tel.: +1-434-982-3578; fax: +1-434-982-1616.

E-mail address: llt2e@virginia.edu (L.K. Tamm).

¹ Class II fusion proteins such as those found in flaviviruses and alphaviruses have a different architecture. They consist of mostly β -structured dimers that lie flat on the viral membrane where they assemble into an icosahedral scaffold [45–47]. Class II fusion proteins have small polypeptide loops at one end that are thought to serve as fusion peptides. The mechanism of fusion of class II fusion proteins is much less well understood than that of class I fusion proteins and is not reviewed here.

long core helices, dissociate from the core structure and extend the original core helices at their N-terminal ends to form long new continuous helices at the top. This major refolding reaction redirects the free N and C termini of the soluble portion of the HA2 chain from the bottom (C-terminal) to the top (N-terminal) end of the long triple coiled coil where they form a hydrogen-bonded threefold symmetric cap structure [7].

The energetics of the refolding of the HA2 core particle has been determined [8–10]. From these studies it became clear that the pH 5 core structure is at a lower energy than the pH 7 structure and that the refolding reaction is essentially irreversible. The pH 7 structure is a kinetically trapped metastable structure that can release stored energy only upon lowering the activation energy that is associated with the structural transition. The activation energy can be lowered by exposing the molecule to pH 5 or high temperatures. It is a common assumption that the energy that is stored in the pH 7 structure contributes to the force that drives membrane fusion. This part of the fusion mechanism has been termed “spring-loaded” [8] because release of the proteinaceous clamp that holds the pH 7 structure in the metastable state leads to the complete inversion of the helices and thus the re-orientation of N- and C-terminal ends of HA2.

What happens in solution in between the two membranes that are to be fused is obviously only one aspect of the mechanism that leads to membrane fusion. Another important aspect deals with the structures and interactions with lipid bilayers of the hydrophobic domains of HA, namely the so-called “fusion peptide” at the N-terminal end and the transmembrane (TM) domain at the C-terminal end of the HA2 polypeptide chain. In order to obtain suitable crystals, these hydrophobic domains have been removed from the core structure that was crystallized at pH 5. The crystallographically determined structure of HA2 at pH 5 comprises residues 34 to 185 [7]. However, the fusion peptide extends from residue 1 to residues 20–24 and the TM domain comprises residues 185–208 of HA2. While the TM domains constitutively anchor HA in the viral membrane, the fusion peptides are shielded in hydrophobic crevices between the HA subunits in the pH 7 structure. They become exposed to membranes only after the low-pH-induced conformational change [11,12]. In this review, I summarize what is known about the structures of HA fusion peptides and TM domains in membranes and then proceed to energetic considerations of fusion peptide–membrane interactions. I will briefly review some biochemical and biophysical evidence for possible roles of the ectodomains in membrane interactions and will finally propose a new model for fusion that is based on these collective results.

2. Structures of fusion peptides in membranes

The “fusion peptide” refers to a moderately hydrophobic sequence of approximately 20 residues that is present in all

viral fusion proteins and that is capable of inserting into the lipid bilayer of the target membrane when the fusion protein is activated. These sequences are usually highly conserved among different strains of the same virus. Even very conservative single point mutations have been shown to ablate fusion of many viral fusion proteins. Fusion peptides are generally rich in glycines and, in some cases, alanines. These residues endow the fusion peptides with an unusual conformational flexibility as will be discussed in more detail further below. This flexibility is a hallmark of fusion peptides and may very well be important for their function. The fact that fusion peptides may exist in different conformations is probably also the reason for many conflicting results that can be found in the relevant literature. Environment and exact experimental conditions can markedly affect the observed structures and, therefore, care should be taken when results from different laboratories are compared.

As is true for the majority of, but not all, viral fusion peptides, the fusion peptide of influenza HA is located at the extreme N terminus of the fusion-promoting subunit, i.e. the HA2 chain in the case of the influenza fusion protein. The influenza fusion peptide comprises 20–24 residues as defined by the apolar/polar residue boundary. The fusion peptide is then followed by nine polar residues, which, although present in the protein that was crystallized at pH 5, do not adopt any ordered structure in these crystals [7]. Therefore, the fusion peptide likely constitutes an independently folded domain of the fusion protein when it inserts into the membrane. The structure of this domain is stabilized and defined by interactions with the lipid bilayer. Therefore, the fusion peptide is sometimes also called the “fusion domain” of the fusion protein.

Early circular dichroism (CD) experiments of synthetic peptides comprising the first 20 residues of HA2 indicated that the influenza fusion peptide is about 50% helical in lipid bilayers or other apolar environments [13–15]. Gray et al. [16] showed that a 23-residue HA fusion peptide adopts a small amount (20–30%) of β -structure in addition to the predominantly α -helical structure. The relative contents of α - and β -structures are strongly dependent on even small details of the sequence, with some sequences that do not promote fusion in the context of the full-length proteins showing much higher contents of β -structures. Polarized Fourier transform infrared (FTIR) spectra showed that the helical segments of the 23-residue peptide are, on average, oriented approximately 50° from the membrane plane [16]. Ishiguro et al. [17] prepared a more soluble 20-residue analog of the influenza fusion peptide, called E5, in which glycines 4 and 8 and threonine 15 were replaced by glutamate residues. This peptide is also predominantly helical, promotes lipid mixing in a pH-dependent manner as the wild-type sequence, and has its α -helical components oriented $\sim 20^\circ$ from the membrane plane. Lüneberg et al. [18] report an average angle of $\sim 45^\circ$ from the membrane plane for the helical components of the 20-residue wild-type peptide sequence. Apart from differences in peptide se-

quence, the methods of sample preparation are also quite different in these studies. Since the native peptide sequences are not or only sparingly soluble in water, they are usually combined with lipids in organic solvent and the complexes are rehydrated after solvent removal. Especially for conformationally flexible peptides, this procedure does not always lead to equilibrium structures in membranes as has been amply demonstrated for another hydrophobic peptide, i.e. gramicidin A [19]. In addition, some investigators prepare multilayers of only partially hydrated films of lipid to record polarized FTIR spectra. The absence of bulk water in these membrane preparations may adversely affect the secondary structures and orientations of amphipathic fusion peptides that reside at the membrane/water interface.

To eliminate these potential sources of error, we have recently developed “second-generation” fusion peptides, which are linked at their C terminus to a polar carrier peptide via a flexible linker [20]. Because the fusion peptide is most likely an independent folding domain in membranes and because the linker to the peptide is designed to be flexible, we believe that the presence of the carrier peptide does not (significantly) affect the structure and membrane interactions of the fusion peptide proper. This general design was highly successful to determine high-resolution structures of various analogs of the influenza fusion peptide in detergent micelles and lipid bilayers. The sequence of the 20-residue wild-type fusion peptide (P20) and the linked polar carrier or host peptide (H7) is

P20H7: GLFGAIAGFIENGWEGMIDG



An initial characterization of this peptide, which is soluble in water at quite high concentrations, by CD and FTIR spectroscopy shows that it is $\sim 90\%$ random coil in solution and $\sim 48\%$ (= 13 residues of P20, H7 is unstructured) helical in lipid bilayers [20]. P20H7 and other host-guest fusion peptides bind to model membranes from aqueous solution, i.e. they can be delivered to membranes as they presumably would be in vivo. The average orientation of the helical segments is $\sim 33^\circ$ from the membrane plane as determined by polarized FTIR spectroscopy of fully hydrated single supported bilayers [20]. Not only is this average angle smaller than what has been measured before with the same methods for the fusion peptide without the linked host peptide, but the standard error of the measurement is also much smaller with the solubilized peptide. The peptides delivered from solution probably find a narrower energy minimum and likely reach equilibrium, whereas multiple conformations may be present and kinetically trapped when the peptides are delivered from organic solvents.

With the new peptide design, their atomic structure in detergent micelles in solution could be determined by NMR spectroscopy [21]. In these experiments, P20H7 was bound

to perdeuterated dodecylphosphocholine (DPC) micelles at a ratio of 1:100. The structures were then solved by ^1H -NMR at pH 7 and pH 5 as shown in Fig. 1. Both structures are characterized by a well-defined N-terminal α -helix that extends from residue 2 to residue 10. Residues 11, 12, and 13 form a turn and redirect the polypeptide chain by about 60° so that it forms a “V” with an opening angle of about 120° . The C-terminal arm does not form a regular secondary structure at pH 7, but forms a short 3_{10} -helix comprising residues 14–18 at pH 5. The N-terminal helix is amphipathic with all bulky hydrophobic residues on the inner side and a ridge of conserved glycines on the outer side of the angled structure. The open C-terminal arm of the pH 7 structure is *not* clearly amphipathic. Polar and apolar residues project to the inside and outside. However, folding of the C-terminal 3_{10} -helix induces an amphipathic structure in this arm as well: Glu 15 and Asp 19 move from the inside to the outside and Met 17 moves to the inside of the “V”. Folding of the C-terminal 3_{10} -helix therefore creates a completely hydrophobic pocket filled with many bulky aromatic residues in the cavity of the “V”.

Two NMR structures of the “E5” peptide, which contains five glutamates (see above), are also available [22,23]. Although the details are different, some general aspects of these two structures are similar to those of the native fusion peptide. Both structures, one in DPC and the other in SDS micelles, consist of two well-ordered helical segments connected by a hinge that extends roughly from Glu 11 to Trp 14 at pH 4–5. Dubovskii et al. [22] report that Glu 11 and Glu 15 have unusually high pK_a 's of 5.6. If confirmed in the native fusion peptide, protonation of these groups may render the outer surface of the “V” less polar and may allow a deeper insertion of the fusion domain into the bilayer (or micelle) at pH 5 than at pH 7. The deeper insertion of the glutamates may induce the folding of the C-terminal 3_{10} -helix, render this segment more amphipathic, and thereby facilitate the insertion of the entire structure deeper into the membrane.

Detergent micelles are much more curved and much more dynamic assemblies than lipid bilayers. It is therefore of interest to know whether the structures that were determined by NMR in detergent micelles are representative of the structures of these peptides in lipid bilayers. To address this question, we have determined the structures of P20H7 in lipid bilayers by spin-label EPR spectroscopy at pH 7 and pH 5 [21]. All 20 residues of the fusion peptide were individually labeled with a nitroxide spin label. Spin labeling Gly 4 and Gly 8 altered the structure of the fusion peptide. Spin labels in the other 18 positions did not appear to have a major perturbing effect on the fusion peptide structure as judged by CD and FTIR spectroscopy. The position of each of these 18 residues in lipid bilayers was then determined by power-saturation EPR spectroscopy in the presence of O_2 , N_2 , and a Ni complex [24]. The final result of these experiments is shown in Fig. 2A. The dispositions of residues in the lipid bilayer have striking similarities to the NMR structures in

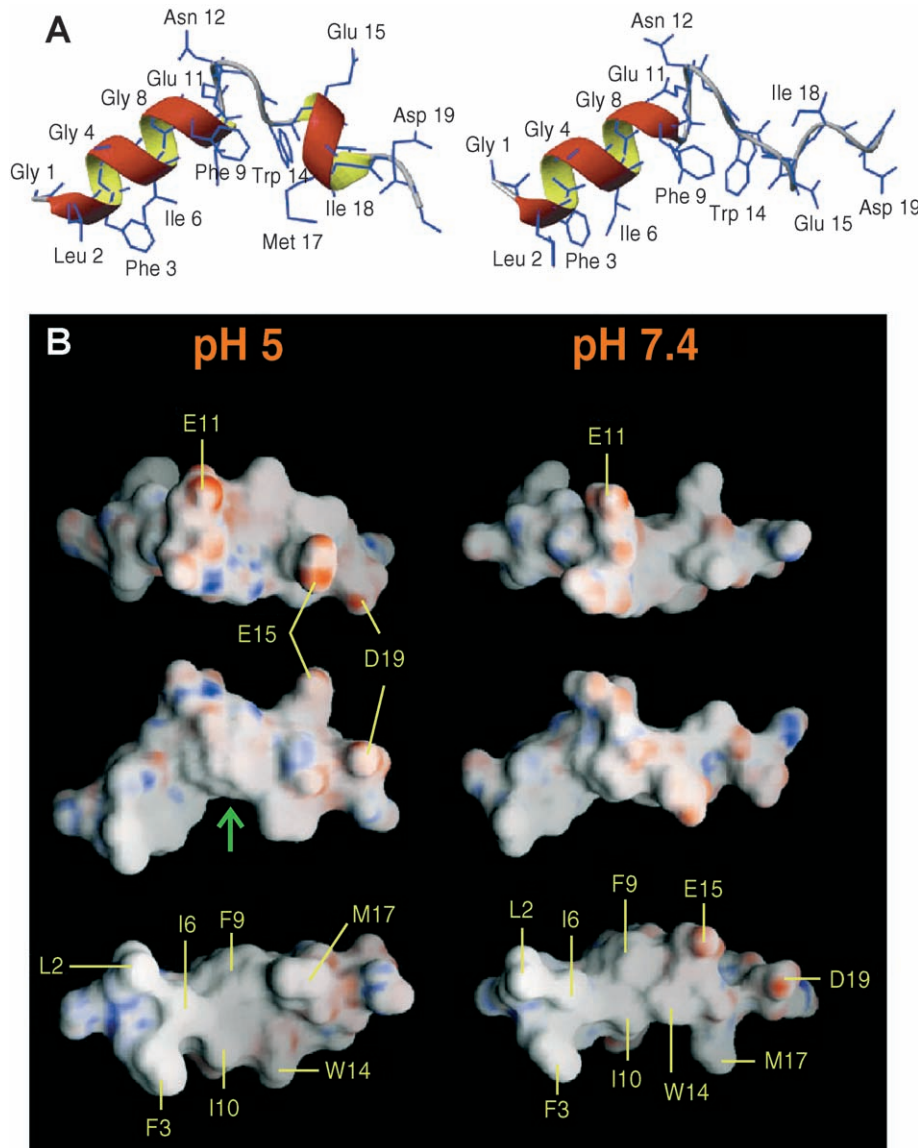


Fig. 1. Structures of influenza hemagglutinin fusion peptide determined by NMR in DPC micelles at pH 5 (left) and pH 7.4 (right). (A) Ribbon representations. (B) Surface potential representations of top view (top), side view (middle), and bottom view (bottom). Red represents negative and blue positive surface potentials. The green arrow points to the hydrophobic pocket in the pH 5 structure (adapted from Ref. [21]).

micelles, both at pH 7 and pH 5. The periodic pattern of a helix extending between residues 1–11, the kink, as well as the C-terminal helix are evident in the EPR structure at pH 5. The more extended C-terminal arm at pH 7 is also apparent. Therefore, it is reasonable to assume that the structures in lipid bilayers are very similar to those in detergent micelles at pH 7 and pH 5.

In addition, the EPR structure defines the angle between the N-terminal α -helix and the membrane plane. This angle is 23° at pH 7 and 38° at pH 5. The 38° determined by EPR for the N-terminal arm is in good agreement with the 33° previously determined by polarized FTIR for the average of the whole peptide [20]. The agreement between two completely different methods of orientation determination validates both methods as well as the optical constants that have

been used to extract the order parameter from the measured FTIR dichroic ratios. The EPR data further show how deep the peptide penetrates the lipid bilayer. The EPR constraints can be used to dock the NMR structures at the membrane interface. The structures shown in Fig. 2B indicate that the C α of Asn 12, which forms the apex in both structures, is coplanar with the average phosphorus position of the phospholipids at both pH values. The N terminus is seen to penetrate about 6 Å deeper into the bilayer at pH 5 than at pH 7. If side chains are included the deepest residues (Leu 2 and Phe 3) reach about 16–17 Å (measured from the lipid phosphate groups) into the proximal leaflet at pH 5, i.e. almost to the mid-plane of the lipid bilayer. Of course, these structures as well as that of the lipid bilayer should be viewed as highly dynamic structures with quite large verti-

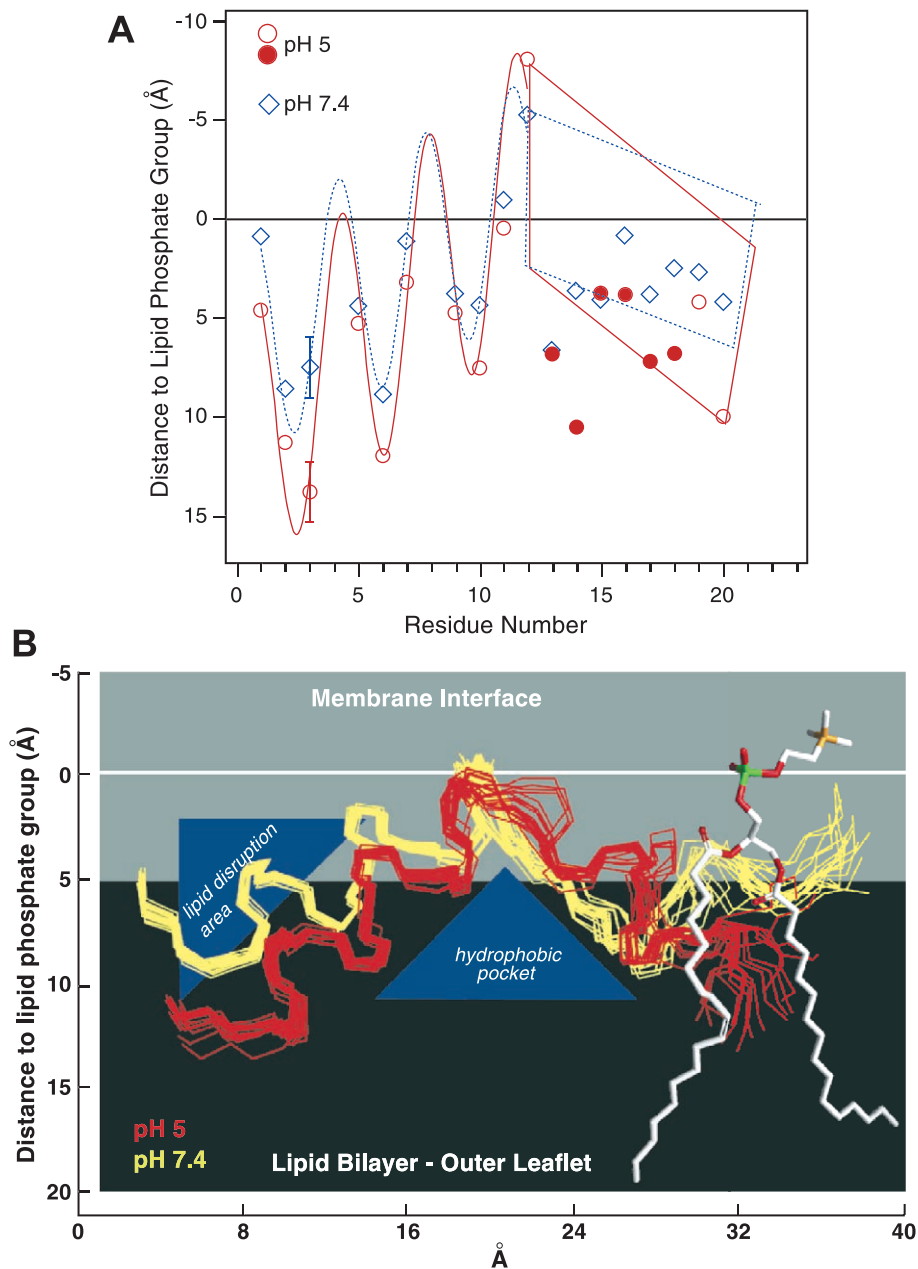


Fig. 2. Position of influenza hemagglutinin fusion peptide in lipid bilayers at pH 5 (red) and pH 7.4 (blue or yellow). (A) Distance measurements of residues by power-saturation spin-label EPR spectroscopy. The same kinked structures with N-terminal α -helical arms are seen as observed by NMR in detergent micelles. (B) High-resolution NMR structures docked to the EPR distance constraints in lipid bilayers. A phospholipid is drawn on the same scale for reference (adapted from Ref. [21]).

cal fluctuations of the lipids and peptide [25]. Future molecular dynamics calculations will likely shed some interesting new light on the dynamics of these assemblies.

The structures of two functionally important fusion peptide mutants have also been determined by NMR in detergent micelles. The G1S mutation causes full-length HA to promote “hemifusion”, but not full fusion [26]. “Hemifusion” is thought to be an intermediate state on the path to full fusion and is operationally defined by a state in which fluorescent lipid dyes exchange between two closely apposed membranes, but fluorescent aqueous dyes do not

communicate across a fusion pore. In full fusion, lipid and contents markers exchange between HA expressing and target cells. The G1V mutation blocks fusion completely so that it does not even proceed to the hemi-fused state [26]. The NMR structure of G1S is very similar to that of the wild-type P20H7 peptide (Fig. 3A). It still forms an angled amphipathic structure with all bulky apolar residues sequestered into the hydrophobic pocket of the “V”. Only the glycine ridge on the outer surface of the N-terminal helical arm is disrupted. In contrast, the NMR structure of G1V shows a very irregular approximately linear amphipathic

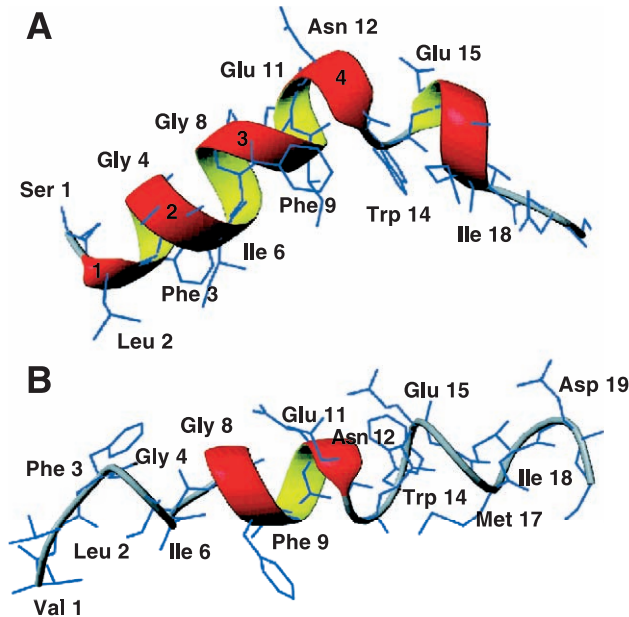


Fig. 3. Structures of G1S (A) and G1V (B) mutant influenza hemagglutinin fusion peptides determined by NMR in DPC micelles at pH 5 (X. Han and L.K. Tamm, unpublished results).

helix (Fig. 3B). Polarized FTIR studies indicate that this helix is oriented approximately parallel to the membrane surface. Based on the structures of these two mutations, it appears that an angled and thus deeply membrane inserted structure is necessary, but not sufficient to promote membrane fusion.

3. Folding and insertion of fusion peptides in membranes

Because P20H7 is water-soluble, the thermodynamics of membrane binding could be studied in quite some detail. As is true for other amphipathic peptides, membrane insertion is coupled to folding of the fusion peptide. We studied the binding of P20H7 and several shorter influenza fusion peptide analogs (P8H7, P13H7, P16H7) to lipid bilayers by a fluorescence method using NBD-labeled analogs of these peptides [20]. Contributions that are due to the electrostatic attraction of the positively charged peptides to the negatively charged bilayers are eliminated by applying a Boltzmann factor weighted by the electrostatic surface potential to the measured binding constant. The electrostatic surface potential is calculated at each peptide concentration from the Gouy–Chapman theory of the diffuse ionic double layer near charged surfaces. The resulting intrinsic binding/partition constant K_o is then used to calculate the free energy of binding

$$\Delta G = -RT \ln(55.5K_o).$$

The factor 55.5 is the molarity of water at 25 °C and accounts for its cratic contribution to the free energy of

binding. Finally, the contribution of the host peptide H7 is subtracted by measuring its binding to lipid bilayers and calculating

$$\Delta\Delta G = \Delta G(\text{PnH7}) - \Delta G(\text{H7}) \quad (n = 8, 13, 16, 20)$$

Fig. 4 shows that all values of $\Delta\Delta G$ are negative and decrease approximately linearly with increasing peptide length. Not surprisingly, increasingly more free energy is gained as the peptide gradually “grows” into the lipid bilayer. Fig. 4 also shows that the negative free energy of G1S is not much reduced, but the negative free energy of G1V is greatly reduced compared to that of the wild-type fusion peptide. This indicates that G1S likely inserts almost as deep as the wild-type peptide into lipid bilayers, whereas G1V is likely more surface-located. These results are consistent with measurements of helix orientation obtained by polarized FTIR spectroscopy. The G1S and wild-type peptide orientations are oblique and very similar to each other, but the helix of G1V is oriented parallel to the membrane plane.

The enthalpies of binding of these peptides to lipid bilayers have been studied by isothermal titration calorimetry (ITC) [27]. Values of $\Delta\Delta H$ have been obtained in much the same way as $\Delta\Delta G$, namely by subtracting the contribution of the host peptide from those of the host-guest fusion peptides. Knowing the free energies and enthalpies of binding, the entropies of binding can be calculated from

$$\Delta\Delta G = \Delta\Delta H - T\Delta\Delta S$$

These values are also plotted in Fig. 4. For all peptides, the enthalpies are *more negative* than the free energies. Therefore, binding of the fusion peptides to small unilamellar vesicles is driven by enthalpy and opposed by

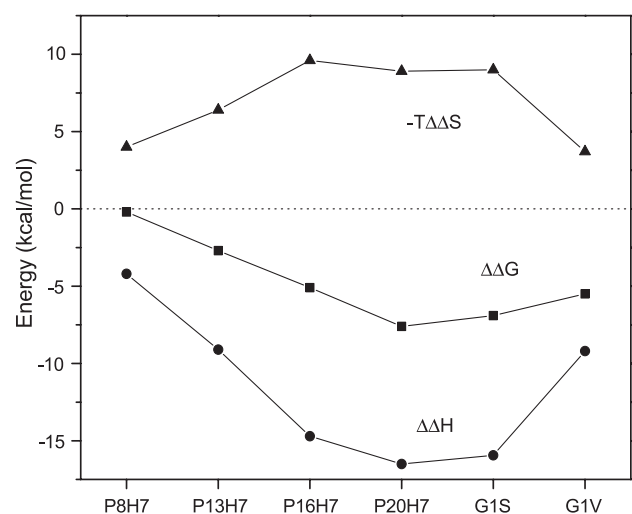


Fig. 4. Free energies, enthalpies, and entropies of influenza hemagglutinin fusion peptide binding to lipid bilayers of POPC/POPG (4:1) at 25 °C. Entropies were converted into energy units by multiplication with -298 K. P8H7...P20H7 refer to fusion peptides of increasing lengths. G1S and G1V are position-1 point mutations of P20H7 (from Ref. [27]).

entropy. This result is opposite to what would be expected if the classical entropy-driven hydrophobic effect were the major driving force for binding and inserting fusion peptides into lipid bilayers. In contrast, binding of fusion peptides to lipid bilayers is driven by enthalpy. It should be noted, however, that this result may only apply to highly curved membranes. Other peptides have been shown to bind to SUVs with a large negative enthalpy, but to LUVs with a positive enthalpy, although the free energies of binding were approximately the same in SUVs and LUVs [28]. Membrane curvature may thus determine whether binding is enthalpy- or entropy-driven. At least in SUVs, the binding of the fusion peptides is associated with a negative entropy change and thus the entropic contribution to the free energies is positive for all peptides of varying length and sequence (Fig. 4). About 50% of the enthalpy of binding is due to folding and another 50% is due to membrane insertion [27]. Thus, formation of the V-shaped fusion domain structure and its deep insertion into the lipid bilayer contribute about equally to the energetics of membrane fusion.

Fusion peptides self-associate at membrane surfaces at high concentrations [29]. This is evident from binding isotherms that deviate in shape from the simple isotherms that would be expected for partitioning as monomers into lipid bilayers. The onset of this effect depends on the specific sequence, but for the wild-type fusion peptide P20H7 starts at about 1 peptide per 300 lipids at pH 5 and about 55 mM ionic strength [29]. FTIR spectroscopy shows that the self-associated peptides adopt an antiparallel β -sheet conformation. The self-association of α -helical monomeric fusion peptides into oligomeric associated β -sheets is reversible. Binding to lipid bilayers in both forms is also reversible. Finally, unstructured fusion peptides aggregate at intermediate to high ionic strength into β -structured oligomers in solution. Taken together, these observations of the different forms of the fusion peptide in solution and in membranes combine to the thermody-

amic cycle depicted in Fig. 5. The equilibrium of the non-fusogenic mutant G1V is strongly shifted towards the antiparallel β -sheet form in membranes. G1S is intermediate between wild-type and G1V with regard to this equilibrium. Therefore, it appears that the fusogenic form is the helical form, whereas excessive self-assembly and β -sheet formation at the membrane surface is inhibitory to fusion. Although the helical form is likely the fusogenic form, a controlled proportion of fusion peptides in the β -sheet form may have a functional role at some stage in fusion, for example by facilitating the assembly of trimers into oligomeric fusion sites.

4. Structure of TM domains in membranes

The structure of the TM domain of influenza HA has been studied by CD and polarized FTIR spectroscopy in detergent micelles and lipid bilayers [30]. As expected, it is highly helical in both environments. At least 19 residues are helical in bilayers of the zwitterionic lipid DMPC. More α -helix (up to 27 residues) is induced, when the peptide, which is flanked by positively charged residues at both ends, is reconstituted into negatively charged bilayers of DMPG. Polarized FTIR experiments show that the peptide is oriented perpendicular to the membrane plane. At low peptide concentrations, the helix axis deviates not more than 15° from the membrane normal. When the peptide/lipid molar ratio is increased to 3.7%, the orientation angle increases to 12 – 26° . Polyacrylamide gel electrophoresis experiments indicate that the HA TM peptides have a tendency to form oligomers in SDS micelles. Dimers, trimers, and tetramers are found. Therefore, it is possible that in the native HA structure, which is a trimer, the TM domains also associate to form trimers. Finally, amide hydrogen-exchange experiments indicate that the TM domains in lipid bilayers are quite accessible to water. These observations are consistent with the TM domains forming oligomers, perhaps even water-accessible pores, in lipid bilayers. One face of the modeled TM α -helix contains several conserved serines and cysteines, which are likely shielded from lipid contacts and perhaps define a water-accessible channel along the center of the oligomer.

5. Roles of the ectodomains in membrane fusion

The pH-triggered “spring-loaded” conformational change of the ectodomain of influenza HA [8,9] was described in the introduction. Energy is released upon refolding of the coiled-coil α -helices. The pH 5 conformation also places the N and C termini of the ectodomain and thus the fusion and TM domains in close spatial proximity to each other. How does this structure and possible intermediates on the path to the final pH 5 structure fit in between the two membranes that are to be fused? How

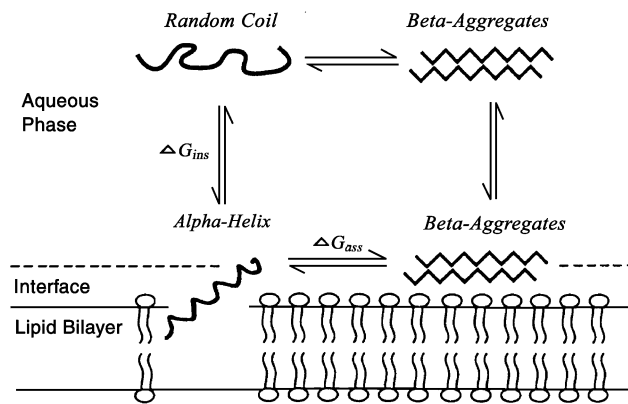


Fig. 5. Thermodynamic cycle for the insertion, folding, and self-association of influenza hemagglutinin fusion peptides in lipid bilayers (from Ref. [29]).

are these structures coupled to the process of membrane fusion? Some insight into the structural role of the ectodomains in membrane fusion comes from polarized FTIR experiments of full-length HA and some of its fragments [31–34]. The helical coiled coils of strain A/PR/8/34 HA are tilted by a large angle at pH 5, but approximately upright at pH 7 [31]. If the fusion peptide inserted into the target membrane before or during tilting, the tilting would provide a mechanism to pull the target and viral membranes into close proximity. The height of the HA trimer and therefore the distance between the two membranes to be fused is about 13 nm at pH 7. A 70° tilt reduces this distance to about 4 nm, i.e. to a range where membrane–membrane interactions become effective. The HA tilt is reversible in the absence of target membranes, but irreversible in their presence [32]. Therefore, tilting may not be a protein-driven process, but rather a membrane-driven process. A possible scenario is that the upright conformation at pH 7 is held in place by a protein clamp, which is released at pH 5. The clamp may be reattached in the absence of target membranes, but removed from interaction with the core protein in the presence of target membranes, if the clamp interacts with these membranes. Possible candidates for the proposed clamp could be parts of the HA1 domain, which have been shown to interact with lipid bilayer model membranes [34]. Another region of the ectodomain that interacts with model membranes comprises the turn residues that connect the major core helices with the antiparallel packed helices at pH 5 [35,36]. Biochemical evidence for reversible refolding steps in HA-mediated fusion support these ideas [37]. The tilting has been confirmed with strain X:31 HA and extended to various of its fragments [33]. Tilting of the coiled coils implies a hinge at the base of HA, i.e. near the TM domain. Using fragments lacking the TM domain, but inserting into model membranes via the fusion peptide, a second hinge between the fusion peptide and the ectodomain has been identified [34]. Several studies using a variety of different approaches have found that several HA trimers act in concert at a single fusion site [38–41]. Fusion is therefore a cooperative process with respect to HA. After inserting the fusion peptides into the target membrane, several trimers tilt presumably simultaneously towards each other, pull the membranes to be fused into close proximity, and thereby establish a precursor of the fusion pore.

6. Spring-loaded boomerang model of viral membrane fusion

Combining the results obtained with the ecto-, fusion, and TM domains, we propose the following “spring-loaded boomerang” model of influenza HA-mediated membrane fusion. Although some elements of this proposal have not yet been experimentally confirmed, the model serves as a working hypothesis to guide the design of future experi-

mentation. In this model, we envision the following sequence of events leading to HA-mediated membrane fusion: (1) The pH change leads to the extrusion of the fusion peptides from the protective hydrophobic crevices in the pH 7 structure of the ectodomain. (2) The coiled coils of HA2 extend towards the target membrane. (3) The fusion peptides insert into the target membrane where they adopt the V-shaped “boomerang” structure shown in Fig. 1 and schematically depicted in Fig. 6 (panel A). Steps 2 and 3 are exothermic. Energy is gained by forming the extended coiled coils and by inserting the fusion peptides into the lipid bilayer of the target membrane (Fig. 4). This energy can be expended on dehydrating and possibly bending the membranes that are to be fused. (4) Several HA trimers assemble to form a single fusion site. Potentially, this assembly could be driven by the self-assembly of fusion peptides in the membrane (Fig. 5). However, the timing of the assembly of HA trimers in physiological membrane fusion is not known. (5) The ectodomains tilt towards the plane of the viral and target membranes (Fig. 6B). This lateral excursion of the ectodomains is likely coupled to the induction of the tight turns between the long coiled coils and the short antiparallel C-terminal helices observed in the pH 5 structure. The structural change brings the fusion and TM peptides into close proximity and the tilting lets the two membranes approach each other. The net effect is a retrieval of the boomerang to a position close to from where it was initially released. It is not yet known whether this retrieval is driven by membrane or protein interactions, or both. (6) Dehydration and possibly other perturbations of the target and viral membrane [30,42] will further decrease the distance between the two membranes to the extent that the lipids of the two proximal leaflets begin to mix. This is the hemi-fused state. We envision this state to be a rather dynamic state, in which the lipids do not adopt a well-defined orientation. The fusion (and perhaps the TM) peptides may act like lipid “mixers” at this stage (Fig. 6B). (7) We propose that a direct interaction between the fusion and TM peptides is required to open the fusion pore. This has already been suggested based on the observation of the capped crystal structure of the ectodomain at pH 5 [7] and is reinforced by the fact that independent mutations in the fusion and TM peptides lead to the same hemifusion phenotype [26,43]. The interaction between the TM domain and the fusion peptide probably requires the conserved glycine ridge on the upper face of the N-terminal arm of the fusion peptide structure. Helix–helix interactions in membranes are often mediated by glycine-rich helical surfaces, as shown, for example, in the structure of the glycophorin A dimer [44]. To actually open the fusion pore, the fusion peptides whose N-terminal arms are too short to span the membrane are hypothesized to slide down the TM domains using them as guiding rails and thereby open their own angled (boomerang) conformation into a more extended membrane spanning helix. The fusion peptides and TM domains of several, perhaps even a large number of HA

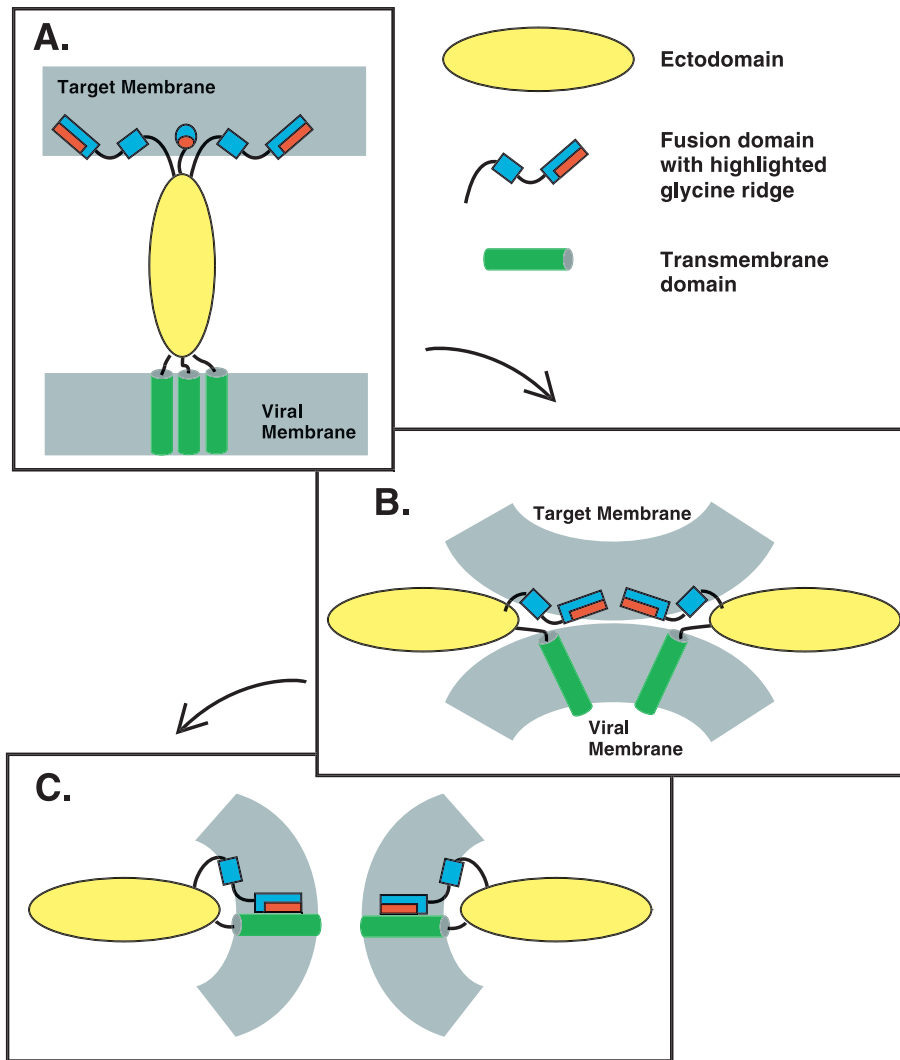


Fig. 6. Boomerang model of influenza hemagglutinin-mediated membrane fusion. (A) The pH-induced conformational change in the ectodomain thrusts the boomerang-shaped fusion peptides towards the target membrane where it inserts. (B) The ectodomains tilt relative to the plane of the membranes. The boomerangs retrieve the target membrane and bring it to close juxtaposition with the viral membrane such that lipid exchange (hemi-fusion) can occur. (C) The fusion peptides and transmembrane domains are thought to interact by virtue of the glycine-edge of the fusion peptide in order to open the initial fusion pore.

trimers are thought to be recruited to facilitate this process (Fig. 6C).

7. Some questions for the future

As mentioned, many aspects of the spring-loaded boomerang model are still hypothetical and need to be experimentally verified before this model can be accepted in full. Several important questions need to be answered: Are the coiled coils N-terminally extended before the C-terminal helices are packed antiparallel against the core helices? And related, do the fusion peptides reach the target membrane before the ectodomains tilt? When do HA trimers assemble to form a distinct fusion site? What are the molecular interactions and driving forces that lead to this assembly? How is a symmetric molecule such as HA biased to tilt in a

specific direction? (An appealing possibility is that breaking the symmetry of individual molecules could be facilitated by imposing a new supra-molecular symmetry encountered in the oligomeric fusion complex. This would imply that the fusion complex has to form *before* the molecules tilt.) What intermediate lipid configurations are adopted and what is the geometry of the “hemifusion” intermediate? How do fusion peptides interact with TM domains? What are the molecular contacts, stoichiometries and interaction energies? What is the structural correlate of the pore “flickering” that has been observed in electrophysiological experiments? What is the irreversible switch that finally opens the fusion pore? Why is this initial fusion pore energetically unstable? Why and how does the initial pore dilate and eventually form an unrestricted single membrane around the viral and cellular compartment? Answering these and other challenging questions will likely guide future research that is directed at

uncovering the mechanics of the molecular machine that fuses viral and cellular membranes.

Acknowledgements

I thank the many talented students and postdoctoral research associates who have worked in my laboratory on these problems over the past several years. The work from this laboratory was supported by NIH grant AI 30557.

References

- [1] J.J. Skehel, D.C. Wiley, *Cell* 95 (1998) 871–874.
- [2] I.A. Wilson, J.J. Skehel, D.C. Wiley, *Nature* 289 (1981) 366–373.
- [3] P.A. Bullough, F.M. Hughson, J.J. Skehel, D.C. Wiley, *Nature* 371 (1994) 37–43.
- [4] L. Godley, J. Pfeifer, D. Steinhauer, B. El, G. Shaw, R. Kaufmann, E. Suchanek, C. Pabo, J.J. Skehel, D.C. Wiley, S.A. Wharton, *Cell* 68 (1992) 635–645.
- [5] G.W. Kemble, D.L. Bodian, J. Rose, I.A. Wilson, J.M. White, *J. Virol.* 66 (1992) 4940–4950.
- [6] T. Bizebard, B. Gigant, P. Rigolet, B. Rasmussen, O. Liat, P. Bösecke, S.A. Wharton, J.J. Skehel, M. Knossow, *Nature* 376 (1995) 92–94.
- [7] J. Chen, J.J. Skehel, D.C. Wiley, *Proc. Natl. Acad. Sci. U. S. A.* 96 (1999) 8967–8972.
- [8] C.M. Carr, P.S. Kim, *Cell* 73 (1993) 823–832.
- [9] C.M. Carr, C. Chaudhry, P.S. Kim, *Proc. Natl. Acad. Sci. U. S. A.* 94 (1997) 14306–14313.
- [10] J. Chen, S.A. Wharton, W. Weissenhorn, L.J. Calder, F.M. Hughson, J.J. Skehel, D.C. Wiley, *Proc. Natl. Acad. Sci. U. S. A.* 92 (1995) 12205–12209.
- [11] J.J. Skehel, P.M. Bayley, E.B. Brown, S.R. Martin, M.D. Waterfield, J.M. White, I.A. Wilson, D.C. Wiley, *Proc. Natl. Acad. Sci. U. S. A.* 79 (1982) 968–972.
- [12] P. Durrer, C. Galli, S. Hoenke, C. Corti, T. Glück, T. Vorherr, J. Brunner, *J. Biol. Chem.* 271 (1996) 13417–13421.
- [13] M. Murata, Y. Sugahara, S. Takahashi, S.-I. Ohnishi, *J. Biochem.* 102 (1987) 957–962.
- [14] J.D. Lear, W.F. DeGrado, *J. Biol. Chem.* 262 (1987) 6500–6505.
- [15] S.A. Wharton, S.R. Martin, R.W. Ruigrok, J.J. Skehel, D.C. Wiley, *J. Gen. Virol.* 69 (1988) 1847–1857.
- [16] C. Gray, S.A. Tatulian, S.A. Wharton, L.K. Tamm, *Biophys. J.* 70 (1996) 2275–2286.
- [17] R. Ishiguro, M. Kimura, S. Takahashi, *Biochemistry* 32 (1993) 9792–9797.
- [18] J. Lüneberg, I. Martin, F. Nüssler, J.-M. Ruyschaert, A. Herrmann, *J. Biol. Chem.* 270 (1995) 27606–27614.
- [19] J.A. Killian, *Biochim. Biophys. Acta* 1113 (1992) 391–425.
- [20] X. Han, L.K. Tamm, *Proc. Natl. Acad. Sci. U. S. A.* 97 (2000) 13097–13102.
- [21] X. Han, J.H. Bushweller, D.S. Cafiso, L.K. Tamm, *Nat. Struct. Biol.* 8 (2001) 715–720.
- [22] P.V. Dubovskii, H. Li, S. Takahashi, A.S. Arseniev, K. Akasaka, *Protein Sci.* 9 (2000) 786–798.
- [23] C.-H. Hsu, S.-H. Wu, D.-K. Chang, C. Chen, *J. Biol. Chem.* 277 (2002) 22725–22733.
- [24] C. Altenbach, D.A. Greenhalgh, H.G. Khorana, W.L. Hubbell, *Proc. Natl. Acad. Sci. U. S. A.* 91 (1994) 1667–1671.
- [25] S.H. White, W.C. Wimley, *Annu. Rev. Biophys. Biomol. Struct.* 28 (1999) 319–365.
- [26] H. Qiao, R.T. Armstrong, G.B. Melikyan, F.S. Cohen, J.M. White, *Mol. Biol. Cell* 10 (1999) 2759–2769.
- [27] Y. Li, X. Han, L.K. Tamm, *Biochemistry* 42 (2003) 7245–7251.
- [28] J. Seelig, *Biochim. Biophys. Acta* 1331 (1997) 103–116.
- [29] X. Han, L.K. Tamm, *J. Mol. Biol.* 304 (2000) 953–965.
- [30] S.A. Tatulian, L.K. Tamm, *Biochemistry* 39 (2000) 496–507.
- [31] S.A. Tatulian, P. Hinterdorfer, G. Baber, L.K. Tamm, *EMBO J.* 14 (1995) 5514–5523.
- [32] S.A. Tatulian, L.K. Tamm, *J. Mol. Biol.* 260 (1996) 312–316.
- [33] C. Gray, L.K. Tamm, *Protein Sci.* 6 (1997) 1993–2006.
- [34] C. Gray, L.K. Tamm, *Protein Sci.* 7 (1998) 2359–2373.
- [35] C.H. Kim, J.C. Macosko, Y.-K. Shin, *Biochemistry* 37 (1998) 137–144.
- [36] E. Leikina, D.L. LeDuc, J.C. Macosko, R. Epand, R. Epand, Y.-K. Shin, L.V. Chernomordik, *Biochemistry* 40 (2001) 8378–8386.
- [37] E. Leikina, C. Ramos, I. Markovic, J. Zimmerberg, L.V. Chernomordik, *EMBO J.* 21 (2002) 5701–5710.
- [38] G.B. Melikyan, W.D. Niles, F.S. Cohen, *J. Gen. Physiol.* 106 (1995) 783–802.
- [39] R. Blumenthal, D.P. Sarkar, S. Durell, D.E. Howard, S.J. Morris, *J. Cell Biol.* 135 (1996) 63–71.
- [40] T. Danieli, S.L. Pelletier, Y.I. Henis, J.M. White, *J. Cell Biol.* 133 (1996) 559–569.
- [41] J. Bentz, *Biophys. J.* 78 (2000) 227–245.
- [42] X. Han, D.A. Steinhauer, S.A. Wharton, L.K. Tamm, *Biochemistry* 38 (1999) 15052–15059.
- [43] R.T. Armstrong, A.S. Kushnir, J.M. White, *J. Cell Biol.* 151 (2000) 425–437.
- [44] K.R. MacKenzie, J.H. Prestegard, D.M. Engelman, *Science* 276 (1997) 131–133.
- [45] F.A. Rey, F.X. Heinz, C. Mandi, C. Kunz, S.C. Harrison, *Nature* 375 (1995) 291–298.
- [46] J. Lescar, A. Roussel, M.W. Wien, J. Navaza, S.D. Fuller, G. Wengler, F.A. Rey, *Cell* 105 (2001) 137–148.
- [47] R. Kuhn, W. Zhang, M.G. Rossman, S.V. Pletnev, J. Corver, E. Lenches, C.T. Jones, S. Mukhopadhyay, P.R. Chipman, E.G. Strauss, T.S. Baker, J.H. Strauss, *Cell* 108 (2002) 717–725.